ELSEVIER

Surface Science 377–379 (1997) 931–936

surface science

Electrochemical Cu deposition on thiol covered Au(111) surfaces

Ornella Cavalleri *, Scott E. Gilbert, Klaus Kern

Institut de Physique Expérimentale, EPF Lausanne, CH-1015 Lausanne, Switzerland

Received 1 August 1996; accepted for publication 15 October 1996

Abstract

The electrochemical deposition of Cu on Au(111) surfaces covered by self-assembled thiol monolayers has been followed in situ by electrochemical STM. Monolayers formed by thiols of different chain length have been chemisorbed on gold electrodes. The thiol molecules are organized in a quasi-crystalline structure characterized by a multi-domain ordering. The presence of the organic layer strongly influences the Cu deposition process. Cyclovoltammetry shows the absence of the underpotential deposition peaks observed on bare gold as well as a decrease of the electrochemical current in the overpotential regime. Independently of the chain length, in the UPD region we observe the formation of Cu nanoparticles 2–5 nm in diameter, one Cu atomic layer in height, uniformly distributed at the surface. The Cu cluster density reaches its maximum in the UPD regime. In the OPD region a chain length dependent behaviour is observed. Long thiol monolayers prevent any further growth of already existing clusters while on short thiol covered surfaces an almost 2D growth of Cu is observed.

Keywords: Copper; Electrochemical methods; Gold; Growth; Scanning tunneling microscopy; Self-assembly; Thiols

1. Introduction

Self-assembled monolayers (SAMs) can be advantageously used to modify metal electrodes in order to obtain well ordered and defined electrochemical interfaces, which find applications in basic and applied research fields from charge transfer studies to corrosion inhibition [1]. An interesting and almost unexplored aspect is the possibility to use these films to modify and control the electrocrystallization of metals on the electrode surface. Different studies have been carried on to investigate the influence of organic additives on the morphology of the electrodeposited metal film, but they mainly dealt with organic molecules dissolved in the electrolyte [2–5]. Up to now the study of metal/organic layer/metal systems has mainly dealt with vacuum deposition of metals on a metallic surface covered by an organic layer [6]. Compared to vacuum deposition, electrochemical deposition offers the advantage of an additional control parameter, i.e. the potential of the metal surface. Moreover, electrochemical scanning tunnelling microscopy (STM) allows us to follow in situ the growth of the metallic overlayer as a function of the surface potential.

In this report we describe the results obtained on the electrochemical deposition of Cu on Au(111) surfaces covered by self-assembled monolayers of alkanethiols. We will first discuss the structure of the thiol/Au(111) interface and then we will focus attention on the electrodeposition of Cu on such a surface. Alkanethiols ($CH_3(CH_2)_nSH$, $n=1,...,21$) are known to form well ordered self-assembled monolayers on

* Corresponding author. Fax: +41 21 6933604.

PII S0039-6028(96)01524-5

Au(111) [7–10], which are thermally stable due to the strong S–Au bonding. The molecules are arranged in a $(\sqrt{3}\times\sqrt{3})R30^\circ$ overlayer structure with the alkyl chain axis canted about 30° with respect to the surface normal. We will show that the presence of these organic spacer layers has an inhibitory effect on the electrodeposition of Cu on gold, the strength of which is found to depend on the organic film thickness.

2. Experimental

The thiol monolayers were formed by self-assembly in 1mM alkanethiol solution onto Au(111) thin films on mica. The gold films were epitaxially grown on mica in high-vacuum, flame-annealed in a hydrogen flame, quenched in ethanol and, while still covered by an ethanol drop, transferred into the thiol solution, where they were kept for at least 15 h. After preparation of a self-assembled monolayer the sample was rinsed with ethanol, dried in an argon flow and transferred to the STM where it was imaged under a dry nitrogen atmosphere. For the electrochemical measurements, the samples, immediately after drying in the argon flow, were transferred to the electrochemical cell while covered by a drop of electrolyte. STM measurements were performed with a home-built variable temperature beetle-type STM [11] which was equipped with a proper electrochemical cell to allow in situ electrochemical STM studies.

3. Structure of alkanethiol SAMs on Au(111)

The morphology of a decanethiol covered Au(111) surface is shown in Fig. 1a. The image was acquired at 360 K after the sample had been annealed for three hours at this temperature. Large molecular domains separated by boundaries, which are imaged as depression lines, characterize the surface. Because of the molecular reorganization which takes place during the annealing, the average domain size attains 400–600 Å [12]. Some small holes are still present on the terraces. As already reported [13–15], these holes are vacancy islands in the topmost gold layer, formed during the initial

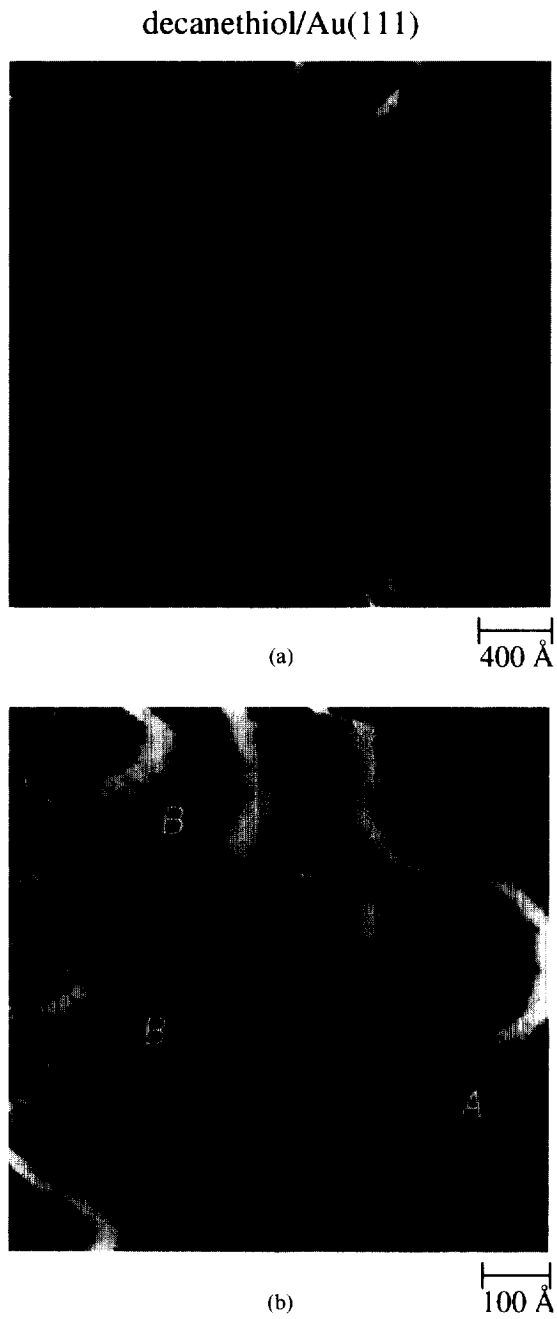

Fig. 1. (a) 3000 × 3000 Å region of a decanethiol covered Au(111) sample annealed for 3 h at 360 K, imaging temperature 360 K; (b) higher resolution image of a decanethiol covered Au(111) surface (810 × 810 Å) annealed for 30 min at 350 K, imaging temperature 300 K. Tunneling parameters: 1.4 V, 0.8 nA.

thiol chemisorption; the holes are covered by molecules as are the surrounding terraces. Annealing has greatly reduced the vacancy island density [15,16] and only a few depressions are left.

By zooming down, the details of the molecular order can be observed as shown in Fig. 1b. In this case, the sample had been annealed for 30 min at 350 K before imaging at 300 K; i.e. the molecular domain size is only 100–200 Å. Two particular structures, labeled A and B, occupy the majority of the surface. Both domains are $c(4\times2)$ superstructures with respect to the $(\sqrt{3}\times\sqrt{3})R30^\circ$ lattice and, according to the model proposed on the basis of the He diffraction data [7], can be explained in terms of different twist patterns of the hydrocarbon chains. Additional uniaxial molecular superstructures have been observed on shorter chain monolayers [17]. The essential feature of the thiol/Au(111) interface which is of importance for the interpretation of the electrodeposition results is the fact that thiols form an ordered, almost defect-free monolayer, which uniformly covers the whole surface. The specific domain ordering of the monolayer is found to be of less importance for Cu electrodeposition on the thiol/Au(111) electrode. As described below, the modification of Cu electrodeposition on covered electrodes caused by the presence of the organic spacer layer is more sensitive to the layer thickness than to the particular kind of molecular pattern.

4. Cu electrodeposition

The electrochemical deposition of Cu on thiol covered Au(111) electrodes has been chosen because of the considerable amount of data available for the Cu/Au(111) system, which serves as a database for investigating the role of the organic layer in the deposition process. It is well known that the electrodeposition of Cu on Au(111) occurs via the formation of a first Cu monolayer in the underpotential region (UPD), i.e. at potentials positive with respect to the Nernstian potential, followed by a 3D bulk deposition of Cu in the overpotential region (OPD), i.e. at potentials lower than the Nernstian potential [18–22]. The presence of the thiol layer strongly modifies the electrodeposition, in the UPD as well as in the OPD region. We followed the process by cyclovoltammetry and by in situ electrochemical STM. Measurements were performed in 0.05M H_2SO_4/1mM $CuSO_4$ electrolyte, and potentials are referred to the Cu/Cu^{++} quasi-reference electrode. Figs. 2a and 2b show the cyclovoltammograms for bare Au(111) and for the same surface covered by a decanethiol monolayer, respectively. Curves similar to the one in Fig. 2b have been found for different chain lengths from hexanethiol up to octadecanethiol. There are two major differences between the two plots. Firstly, in the presence of the organic layer, the deposition and stripping peaks in the UPD region, which are characteristic of bare gold, disappear and, secondly, the measured electrochemical current is one order of magnitude lower in the case of a covered electrode than for bare gold. The absence of the UPD peaks suggests that in the presence of thiols the deposition of Cu does not occur abruptly in a narrow window of potential as on bare gold. Moreover, the decrease in the electrochemical current observed in the presence of thiols shows the inhibitory effect of the organic layer on the deposition.

The structural changes of the electrode surface accompanying the process have been followed in situ by STM. Fig. 3 shows the initial stage of Cu deposition on a decanethiol covered Au(111) surface. The image was acquired at +50 mV versus Cu/Cu^{++}, i.e. at a potential lower than the first UPD peak observed on bare gold. At this potential in the absence of thiols one would observe a complete monolayer of Cu deposited on the surface, while Fig. 3 shows the deposition of isolated nanosized Cu clusters uniformly distributed on the surface. The Cu clusters are 2–5 nm in size, one Cu layer in height and grow randomly on the surface without any preferential nucleation site like steps or holes. The maximum cluster density ($\sim 2\times10^{-4}$ cluster $Å^{-2}$) is reached in the UPD region. By sampling over different regions of the surface it has been observed that the cluster nucleation does not take place simultaneously on the whole surface, but occurs randomly in patches. New clusters then grow around these regions and finally cover the whole surface [23]. One might speculate that the areas where the cluster

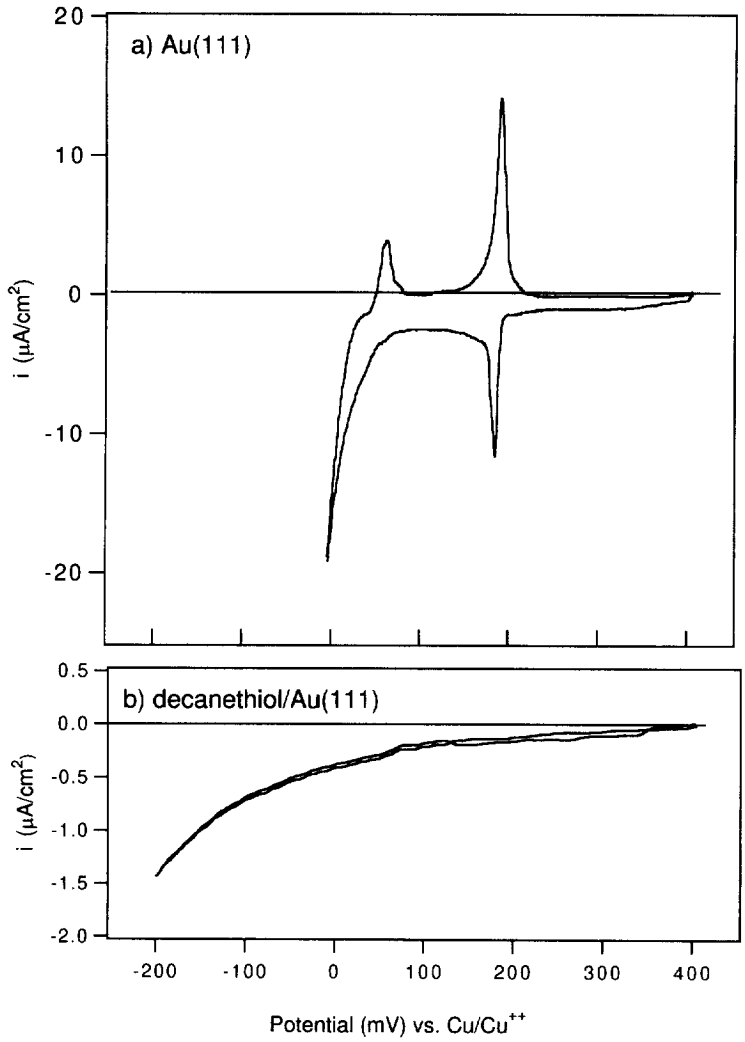

Fig. 2. Cyclic voltammograms of Cu deposition on (a) bare Au(111) thin film on mica and (b) Au(111) film covered by a decanethiol monolayer. Scan rate: 5 mV s^{-1} for both voltammograms taken in nondeaereated 0.05M H_2SO_4/1mM $CuSO_4$.

deposition begins are characterized by poorer order in the thiol monolayer which could facilitate the electron transfer across the layer necessary to reduce the Cu ions. The same scenario characterizes the UPD deposition on gold electrodes covered by thiols of different chain lengths, from 6 to 18 carbon atoms.

As already reported [23], several tens of minutes are necessary to obtain a homogeneous distribution of Cu clusters on the whole surface as shown in Fig. 3. By assuming a compact (1×1) structure for the Cu islands, the deposition rate would correspond to a current of 10 nA cm^{-2}, a value well below the measured dynamic current which can not be detected as a peak in the $I(V)$ curve of Fig. 2b.

A chain length dependent inhibitory effect is observed at potentials corresponding to the OPD for bare gold. For short chain monolayers, decreasing the potential in the cathodic region does not induce any growth of the Cu clusters until overpotentials of several tens of millivolts are reached. It

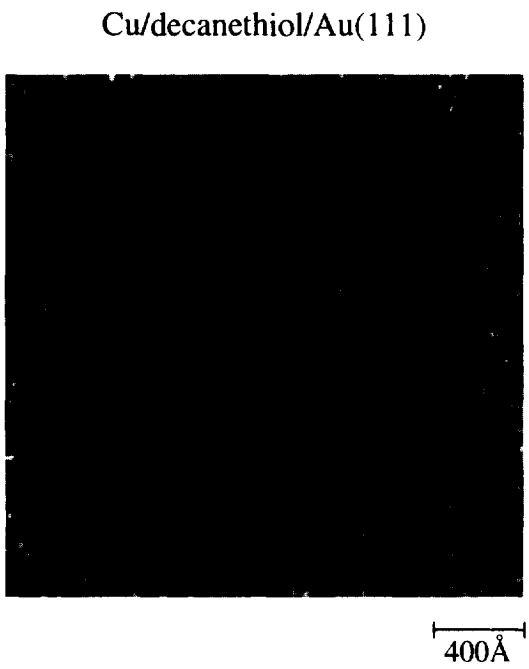

Fig. 3. In situ STM image (2300 × 2300 Å) of a decanethiol covered Au(111) surface decorated with Cu clusters in the UPD region. Electrolyte: 0.05M H_2SO_4/1mM $CuSO_4$, $E = 50$ mV versus Cu/Cu^{++}. Tunneling parameters: 0.10 V, 0.3 nA.

is only at potentials lower than −80 mV that a further development of the deposition is observed. This is shown in the sequence of images in Figs. 4a–c which were taken on a hexanethiol covered Au(111) electrode at −110 mV 20, 50 and 120 min, respectively, after the potential had been reduced to −110 mV. It is interesting to note that the growth mechanism is now completely different with respect to the case of bare gold. Instead of 3D growth, we observe a quasi-two-dimensional growth of Cu. Cu clusters grow in a ramified fashion and finally coalesce to complete the first monolayer. The formation of the second monolayer starts only when the first one is almost complete. Only at potentials as low as −160 to −200 mV is the sudden growth of large 3D Cu nodules observed, probably due to a breakdown of the thiol layer at such negative potentials. The blocking effect of long chain monolayers ($n > 12$) is even more pronounced. In this case, the Cu clusters formed in the UPD region do not undergo any modification or growth even at potentials well

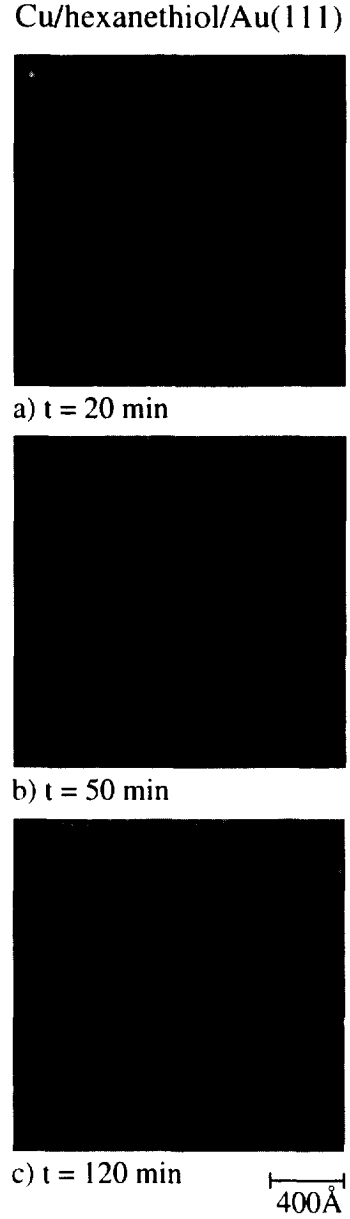

Fig. 4. (a)–(c) Temporal sequence of in situ STM images (1800 × 1800 Å) showing the development of the Cu deposition on a hexanethiol covered Au(111) surface in the OPD region. Electrolyte: 0.05M H_2SO_4/1mM $CuSO_4$, $E = -110$ mV versus Cu/Cu^{++}. Tunneling parameters: 0.12 V, 0.5 nA.

negative in the OPD regime. Octadecanethiol covered electrodes still show isolated Cu nanoparticles even after being kept for some hours at potentials

lower than −150 mV. It is only at about −200 mV that the growth of large Cu nodules is observed. It must be noted that the exact onset potentials for the different processes described, i.e. Cu clusters growth, quasi-2D growth on short monolayers and 3D nodule formation, are characterized by a certain variability for the different chain lengths and for each individual sample.

The highly reduced growth kinetics, together with the stronger growth inhibition caused by thicker monolayers, supports the contention that the Cu electrocrystallization occurs on top of the alkanethiol layer. This view is supported by the conclusions of a similar study [24]. Such a scenario allows us to explain the more efficient blocking effect observed for thicker monolayers by noting that longer molecules produce a thicker and also a more compact monolayer (because of the higher van der Waals interactions between molecular chains), which makes electron transfer across the layer more difficult. As a consequence the reduction of Cu ions to Cu atoms, which needs electrons to be transferred from the gold surface, is limited.

References

[1] Bard, H.D. Abruña, C.E. Chidsey, L.R. Feldberg, K. Itaya, D. Majda, O. Melroy, R.W. Murray, M.D. Porter, M.P. Soriaga and H.S. White, J. Phys. Chem. 97 (1993) 7147, and references therein in conjunction with Section 4 of this review.

[2] R.J. Nichols, C.E. Bach and H. Meyer, Ber. Bungenses. Phys. Chem. 97 (1993) 1012.

[3] A.S. Dakkouri, N. Batina and D.M. Kolb, Electrochim. Acta 38 (1993) 2467.

[4] M.H. Hölzle, C.W. Apsel, T. Will and D.M. Kolb, J. Electrochem. Soc. 142 (1995) 3741.

[5] W. Haiss, D. Lackey, J.K. Sass, H. Meyer and R.J. Nichols, Chem. Phys. Lett. 200 (1992) 343.

[6] D.R. Jung, A.W. Czanderna, CRC Crit. Rev. Solid State Mater. Sci. 19 (1994) 1, and references therein.

[7] N. Camillone, Ch.E.D. Chidsey, G. Liu and G. Scoles, J. Chem. Phys. 98 (1993) 3503.

[8] R.G. Nuzzo, E.M. Korenic and L.H. Dubois, J. Chem. Phys. 93 (1990) 767.

[9] D. Anselmetti, A. Baratoff, H.J. Güntherodt, E. Delamarche, B. Michel, Ch. Gerber, H. Kang, H. Wolf and H. Ringsdorf, Europhys. Lett. 27 (1994) 365.

[10] P. Fenter, P. Eisenberg and K.S. Liang, Phys. Rev. Lett. 70 (1993) 2447.

[11] J.P. Bucher, H. Röder and K. Kern, Surf. Sci. 289 (1993) 370.

[12] O. Cavalleri, A. Hirstein, J.P. Bucher and K. Kern, Thin Solid Films 284/285 (1996) 392.

[13] K. Edinger, A. Golzhauser, K. Demota, C. Wöll and M. Grunze, Langmuir 9 (1993) 4.

[14] J.A.M. Sondag-Huethorst, J. Jorritsma and L.G.K. Fokkink, Langmuir 10 (1994) 611.

[15] J.P. Bucher, L. Santesson and K. Kern, Langmuir 10 (1994) 979.

[16] O. Cavalleri, A. Hirstein and K. Kern, Surf. Sci. 340 (1995) L960.

[17] G.E. Poirier, M.J. Tarlov and H.E. Rushmeier, Langmuir 10 (1994) 3383.

[18] T. Hachiya, H. Hombo and K. Itaya, J. Electroanal. Chem. 3 (1991) 275.

[19] O.M. Magnussen, J. Hotlos, R.J. Nichols, D.M. Kolb and R.J. Behm, Phys. Rev. Lett. 64 (1990) 2929.

[20] Z. Shi and J. Lipkowski, J. Electroanal. Chem. 365 (1994) 303.

[21] M.F. Thoney, J.N. Howard, J. Richer, G.L. Borges, J.G. Gordon, O.R. Melroy, D. Yee, L. Sorensen, Phys. Rev. Lett. 75 (1995) 4472.

[22] W. Haiss, J.K. Lackey and M. van Heel, in: Atomic Force Microscopy/Scanning Tunneling Microscopy, Eds. S.H. Cohen et al. (Plenum, New York, 1994) p. 423.

[23] S.E. Gilbert, O. Cavalleri and K. Kern, J. Phys. Chem. 100 (1996) 12123.

[24] J.A.M. Songad-Huethorst and L.G.J. Fokkink, Langmuir 11 (1995) 4823.